

The Framework for Real-Time Simulation of Deformable Soft-Tissue Using a Hybrid Elastic Model

Shaoting Zhang¹, Lixu Gu^{1,2}, Weiming Liang², Pengfei Huang¹,
Jan Boehm³, and Jianfeng Xu²

¹ School of Software, Shanghai Jiao Tong University
kawaii.tony@gmail.com
<http://www.se.sjtu.edu.cn/igst/>

800 Dongchuan Road, Shanghai, P.R.China, 200240

² Computer Science, Shanghai Jiao Tong University

³ Computer Science, Technische Universitat Berlin

Abstract. In this paper, we present a novel approach for real-time simulation of deformable soft-tissue. The framework includes segmentation of medical data, physical and mathematical modeling, performance optimization as well as collision detection. The physical and mathematical modeling which is the most significant phase in the approach is based on an improved elasticity theory which uses the skeleton structure of the deformable object to reflect volumetric information. We also refine the model to satisfy the real-time computation requirement and achieve a reasonable deformation effect on the global level as well as the local region by introducing the concepts of the angular spring, the return spring and the local deformation concept. A model based on real clinical data using a segmented left kidney and a collision detection demo are presented as an example in our case study.

1 Introduction

Today, most practical surgical training and education is done on living animals, cadavers and high-quality phantom models, all of which are expensive and might relate to ethical problems. Meanwhile, accompanied with the rapid development of medical image processing and soft-tissue modeling technology, virtual surgery appears to be a substitute of traditional training approaches. Thus Virtual Reality (VR) and real-time simulation are important in the biomedical imaging domain.

Numerous scientists have proposed various methods to model soft-tissue in the past years. Nicolas Ayache and INRIA presented a real-time Finite Element Method (FEM) [1] for virtual surgery. Sarah F. developed linked volumes (Mass Spring Systems) [2] to model object collisions, deformation, cutting, caving and joining. Stephen M. Pizer and Kaleem Siddiqi invented the Multi-Scale Medial Loci (M-Rep) [3] to represent the internal information of deformable objects and reconstruct the boundary by medial atoms. Sarah F. also developed 3D

ChainMail [4] which is modeled by complicated calculations on a small number of elements and achieves a fast speed. However, existing methods are still not perfect. Although FEM is accurate enough, it is time-consuming and difficult to implement; Mass Spring Systems could meet with the real-time requirement when the number of mass points are limited [5], but the traditional Mass Spring System does not represent the inner structure appropriately, which might result in the unreasonable appearance under large scale force; M-Rep modeling of the global deformation is effective because of the skeleton structure, but the appearance of the surface is not good; ChainMail is fast enough but does not reflect the physics characteristic of soft tissue.

In our framework, we endeavor to deal with these problems mentioned above. We employ a proper segmentation method to obtain a regular surface mesh structure and establish a Mass Spring model based on the meshes. Then the skeleton of the soft-tissue is extracted by the Distance Mapping Method [6]. After that, the surface model and skeleton are correlated according to specific rules. Finally, the model is refined to reduce response time.

The following sections describe the details of each component in the framework. In section 2 we compare two sorts of surface mesh structures and chose the superior one. Section 3 models the soft-tissue using a hybrid approach. Section 3.3 introduces the local region deformation approach to decrease response time. Finally, we present the experiment results in section 5.

2 Surface Reconstruction

Medical image data supplied by the radiology department of Shanghai Oriental Hospital is used as source of the soft tissue model. In order to extract the organ rapidly and accurately, a Multi-stage Segmentation Approach [7] consisting of the Fast Marching method and Morphological Reconstruction is employed. In the first stage, a structuring element (e.g. a sphere with 1 pixel radius) is used to recursively erode the input 3D image until the Region Of Interests (ROI) is completely separated from the neighboring tissues. In the second stage, the Fast Marching method is employed to rapidly propagate the user-defined seed to a position close to the boundary. Then taking the output of the Fast Marching algorithm as the initial seed, Morphological Reconstruction is employed for refinement. In the final stage, recursive dilation is employed to recover the lost data from the first stage. The Multi-stage approach can make full use of the speed of the Fast Marching method as well as the accuracy of the Morphological Reconstruction algorithm. After the Multi-stage segmentation, Marching Cubes and Balloon Segmentation are employed separately on the segmented kidney to obtain two different surface meshes. Marching cubes is used for surface construction and can produce a triangle mesh by computing iso-surfaces from discrete data. Fig. 1(A) shows the complex mesh topology after the approach. Balloon Segmentation is a volumetric segmentation method based on dynamic deformable meshes [8]. An external image force is applied to an initial simplex mesh and makes the mesh expand or shrink towards the surface of the organ

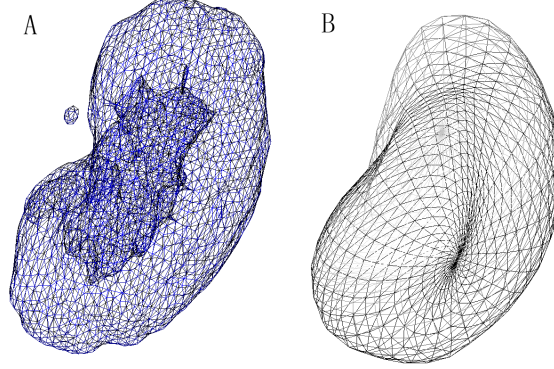


Fig. 1. Two sorts of meshes. (A) The mesh structure obtained by using marching cube. (B) The mesh structure acquired by employing balloon segmentation.

until the simplex meshes meets with the boundary. Fig. 1(B) displays the result of this method.

The former meshing algorithm generates extreme convoluted and irregular meshes with 2824 surface points and 5604 triangles, while the latter method delivers a relatively simple and regular mesh structure with just 994 surface points and 1984 triangles. Moreover, the former mesh topology is hollow and contains many fragments, which could result in the corruption of the mass-spring system under large large forces. Thus the latter mesh is preferred and appropriate for the following modeling process.

3 Soft-Tissue Modeling

We establish a surface model based on the Mass Spring system and employ a simplified M-Rep to represent the internal information. A hybrid elastic system is established by combining the two structures and later polished to reduce the calculation time.

3.1 The Surface Mass-Spring Model

The Mass Spring system models soft-tissue as a set of mass points linked with each other through springs. The topology of masses and springs is described in Fig. 2(A). Fig. 2(B) presents the construction of the fundamental unit of the system: the elastic spring and the damper. The former generates the elasticity force proportional to the change of the springs' length, and the latter provides a damping force proportional to the velocity of the mass points.

The system employs a differential equation to calculate the displacement of the surface points:

$$m_i \cdot \frac{\partial^2 \mathbf{x}_i}{\partial t^2} + d_i \cdot \frac{\partial \mathbf{x}_i}{\partial t} + \sum_{j \in \sigma(i)} k_{i,j} \cdot \delta l_{i,j} = F_i \quad (1)$$

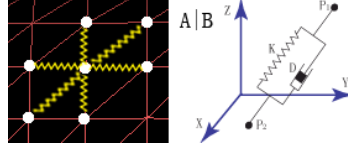


Fig. 2. (A) The topology of masses and springs. (B) The basic component of the Mass Spring system: masses (black dots), damper and spring.

Where m_i , d_i , and F_i are the mass, damping factor and external force of the i th mass respectively. x_i is the $3n$ vector displacement of the i th mass points. σ_i represents the mass points directly linked to the i th mass. $k_{i,j}$ and $\delta l_{i,j}$ denotes the elasticity factor and the length alternation of spring ij respectively. The explicit Euler method [9] is employed to solve formula 1 and computed the force on each node.

In the implementation, the Angular Spring [10] and the Return Spring [11] are introduced to refine and rationalize the deformation appearance. The former is employed to simulate the curvature force [10] which controls the degree of bending and twisting of soft-tissue. The latter is utilized to prevent soft-tissue from escaping from its original location.

3.2 The Skeleton Structure

S.M. Pizer introduced a deformable model (M-Rep) which uses medial atoms and a particular tuple $(\{x, r, F(\mathbf{b}, \mathbf{n}), \theta\})$ [3] to imply the boundary coordinates of soft-tissue. M-Rep is a sound approach to reflect the internal information because each medial atom represents an interior section [11] of the object.

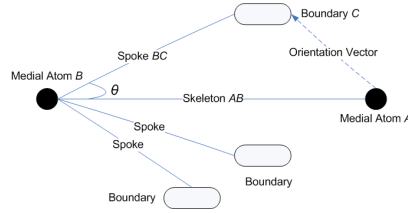


Fig. 3. The topology of the medial atoms and spokes

In the system the improved Distance Mapping Method [6] is employed to extract the skeleton from CT data, along which media atoms are selected evenly and automatically. Then we modify the topology of M-Rep to simulate the hub-and-spoke structure (Fig. 3) and alter the tuple to reduce the calculation time [11]. The tuple is altered to $\{x, r, F(\mathbf{V}, \mathbf{AB}), \theta\}$, where x is the coordinate of the medial atom B ; r is the length of the spoke BC ; $F(\mathbf{V}, \mathbf{AB})$ is the plane

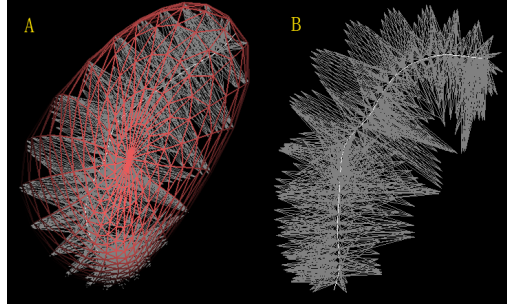


Fig. 4. (A) The hybrid elastic model consisting of surface mesh and internal topology. (B) The internal structure with spokes and the skeleton.

determined by vector \mathbf{V} and \mathbf{AB} ; \mathbf{V} is the Orientation Vector of boundary C which links medial atom A with boundary C ; θ is the angle between skeleton \mathbf{AB} and spoke \mathbf{BC} . The coordinate of boundary C can be calculated by the following formula:

$$\underline{C} = x + R_{\mathbf{V}, \mathbf{AB}}(\theta) \mathbf{AB} \cdot \frac{r_{\mathbf{BC}}}{|\mathbf{AB}|} \quad (2)$$

Where \underline{C} and x are the coordinates of boundary C and medial atom B respectively; R denotes the operator to rotate its operand by the argument angle in the plane spanned by \mathbf{V} and \mathbf{AB} ; $|\mathbf{AB}|$ means the length of the vector \mathbf{AB} . Other spokes connecting with B can be calculated by rotating \mathbf{BC} around \mathbf{BA} and scale the r length. Iterating the process can obtain all boundaries.

3.3 The Hybrid Elastic Model

The surface Mass Spring system (Fig. 1(B)) and the skeleton topology (Fig. 4(B)) are combined in a hybrid elastic model. Firstly, each spoke will be linked with the nearest boundary points ([11]). However this topology is not robust enough due to the single connection between the centerline and each surface point. Thus each boundary point will be connected with the four nearest medial atoms by virtual springs (Fig. 4(A)). By doing this, the hybrid structure holds both the inner and the outer information which ensures a sound deformation effect on global level as well as local.

Finally, an iterative approach [11] is used to obtain the appropriate parameters of the elastic system, such as d , k , m of the inner structure and the outer mesh respectively. The values of the internal parameters should be much larger than the ones on the surface because the volume represented by the inner points is much larger than the one of the outside points.

4 Local Region Deformation

According to hospital statistics, most surgery operations are performed in a small area and the rests of the tissue is nearly stable [12], so we determined to restrict

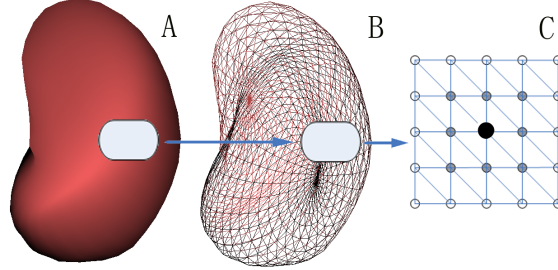


Fig. 5. (A) The local deformation region (the big grey spot) on a left kidney in the solid view. (B) (A) in the mesh view. (C) The topology of the local deformation region (The distance between the center black spot and the grey ones is 1, distance with the white ones is 2).

the deformation to a local level if the external force is relatively small in order to reduce the calculation time.

In the preprocessing stage of the application, the Dijkstra algorithm is employed to calculate the shortest path between all pairs of mass points. A table recording these distances is generated and kept. The lengths of all springs are assigned to be 1 in order to reduce the complexity and computation time. The deformation procedure is the following: if a small force is applied on the local deformation region (Fig. 5(A),(B)) and assuming that the propagation of the force is limited in the second layer, the application will search the distance table to find points whose distance from the black region is not greater than 2 (Fig. 5(C)) and these points will be transformed according to formula 1, while the displacement of other points, such as those marked 3 and 4 in the distance table, will be ignored and not calculated. The mechanism will be skipped when the external force is quite large because most mass points might be influenced under the global scale force.

5 Experiments

The framework is performed on a computer with an Intel Pentium IV-2.80 GHz CPU, 1G byte of ram, and a GeForce 6800 graphics card. The code is compiled with Visual C++ 7.0. There are 994 points on the surface, 48 points on the skeleton, and 256 strips in the surface mesh structure.

Fig. 6 compares the deformation results of the hybrid model with the surface mass-spring model. The hybrid elastic model receives a reasonable appearance on both local and global level (Fig. 6(A), (B), (C)). Fig. 6(A) and Fig. 6(B) also display the effect of collision detection. Fig. 6(D) reveal a unreasonable result of the surface mass-spring models.

Table. 1 displays the computation time of different models. Here local force means that we apply a relatively small force on a surface point, and global force means that a large forces on 10 points is applied. The update rate (including the

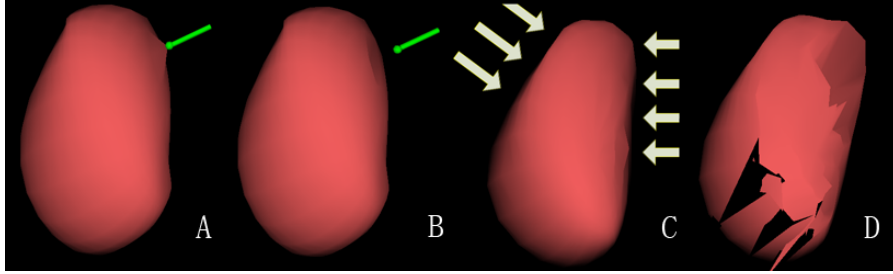


Fig. 6. Deformation effect of the segmented kidney: (A) Nip of the kidney and collision detection based on the hybrid model; (B) Release of the nip and local deformation; (C) Global deformation under large scale force; (D) Surface mass-spring model under large scale forces;

Table 1. Comparison of the calculation time (milliseconds per update time) among different elastic systems. (Surface MS = surface Mass Spring; Volume MS = Volume Mass Spring; Hybrid MS = the elastic system with internal structure; Hybrid LR = hybrid model with Local Region Deformation; LF = local force; GF = global force; 25, 50, 75, 100, 500 = the magnitude of the forces).

ms/update	Surface MS	Hybrid MS	Hybrid LR
LF(25)	0.531	0.766	0.750
LF(50)	0.547	0.829	0.765
LF(75)	0.546	0.812	0.782
LF(100)	0.563	0.859	0.797
GF(500)	1.891	11.187	7.938

rendering time) of the hybrid model with the local region optimization is about 150 times per second under local force and about 30 times under global force. Such rate is more efficient than the one without optimization and meets with the real-time requirement (15-20 times per second).

6 Conclusions

This paper introduced a convenient framework and methodology to model a generic soft-tissue and proposed a hybrid elastic system to simulate the deformation of soft-tissue effectively and efficiently on global level as well as in local regions. Our main contribution is combining the skeleton structure with the surface mesh, confining the deformation region when the external force is relatively small, and bringing in the concept of the return spring, all of which polish the appearance of soft tissue and decrease the response time.

The future work is to model more complicated organs such as the heart. In order to obtain the branches of the complex soft-tissue, the skeleton-extraction

algorithm needs to be improved. Moreover, the medial representation topology and the tuple mentioned in section 3.2 could be used to recalculate the positions of implied boundaries when the coordinates of the skeleton are changed. We endeavor to bring in this recalculation to better mix the advantages of the two models. Our recent work also includes the addition of force feed back equipment into the program.

Acknowledgements

This work was partially supported by the Natural Science Foundation of China, Grant No. 70581171, and the Shanghai Municipal Research Fund, Grant No. 045118045. The authors would like to thank Dr. Pizer (University of North Carolina) for patiently discussing the concept of M-Rep with members of our lab and Dr. Ayache (INRIA) for giving the impressive presentation about virtual surgery at ICCV2005. We also thank Guangxiang Jiang, a member in the Image Guided Surgery Therapy laboratory in SJTU, for developing the application to extract the skeleton of the kidney recorded in DICOM format.

References

1. Cotin, S., Delingette, H., and Ayache, N.: Real-time Elastic Deformations of Soft Tissues for Surgery Simulation. *IEEE Transactions on Visualization and Computer Graphics* (January-March 1999). Vol. 5, NO. 1, pp. 72-83
2. Frisken-Gibson, S.F.: Using Linked Volumes to Model Object Collisions, Deformation, Cutting, Carving, and Joining. *IEEE Transactions on Visualization and Computer Graphics* (October-December 1999). Vol. 5, NO. 4, pp. 333-349
3. Pizer, S.M., Siddiqi, K., and Szekely, G.: Multiscal Medial Loci and Their Properties. *IJCV Special UNC-MIDAG issue*. Vol. 55(2/3): 155-181
4. Sarah, F., Delingette, N., and Ayache, N.: 3D ChainMail: a Fast Algorithm for Deforming Volumetric Objects. *Proc. 1997 Symposium on Interactive 3D Graphics*. pp. 149-154.
5. Conti, F., Khatib, Q., and Baur, C.: Interactive Rendering of Deformable Objects Based on A Filling Sphere Modeling Approach. *Proceedings of the 2003 IEEE International Conference on Robotics & Automation, Taipei, Taiwan (September 14-19, 2003)*
6. Wan, M., and Liang, Z.: Automatic Centerline Extraction for Virtual Colonoscopy. *IEEE Transactions on Medical Imaging* (December 2002). Vol. 21, NO. 12
7. Gu, L., Xu, J., and Peters, T.: A Novel Multistage 3D Medical Image Segmentation: Methodology and Validation. *IEEE Transaction Information Technology in Biomedicine*. (in press)
8. Mitchell, B.R., Sahardi, T.A., and Vision, M.: Real-time Dynamic Deformable Meshes for Volumetric Segmentation and Visualization. In *Proc BMVC 1997*. Vol. 1, pp. 311-319
9. Chen, Y., Zhu, Q., and Kaufman, A.: Physically-based Animation of Volumetric Objects. *Computer Animation 1998*. pp. 154.
10. Nedel, L.P., Thalmann, D.: Real Time Muscle Deformations Using Mass-Spring Systems. *Proceedings of the Computer Graphics International (1998)*. pp. 156-166

11. Zhang, S., Gu, L., and Huang, P.: Real-Time Simulation of Deformable Soft Tissue Based on Mass-Spring and Medial Representation. *Computer Vision for Biomedical Image Applications*, a workshop of ICCV2005. LNCS 3875, pp. 419-427
12. Chai, J.Y., and Sun, J.: Hybrid FEM for Deformation of Soft Tissues in Surgery Simulation. *International Workshop on Medical Imaging and Augmented Reality (2001)*. pp. 298-303